Racemic and Meso Diastereomers of a *P*-Chirogenic Diboranyldiphosphinoethane

Brady J. H. Austen, Harvey Sharma, Joseph A. Zurakowski, and Marcus W. Drover*

Department of Chemistry and Biochemistry, The University of Windsor, 401 Sunset Avenue, Windsor, ON, N9B 3P4, Canada

Abstract: Diphosphine ligands have enjoyed great success as supporting moieties for transition elements, where modification of both primary and secondary coordination sphere has been shown to illicit differences in chemical reactivity. This work describes a new family of such ligands constructed from the previously reported scaffold, (±)-*rac*/*meso*-(*t*-Bu)ClP-CH_2CH_2-PCl(*t*-Bu) that bears bulky *tert*-butyl substituents. Reaction of this precursor with allyl magnesium chloride and subsequent hydroboration using $HBCy_2$ (Cy = cyclohexyl) provides access to a diboranyldiphosphinoethane – the first in a class of ligands having two electrophilic boranes in their secondary coordination sphere. As a testing ground for coordination, these motifs (and their allyl precursor) have been installed at Ni(0) using [Ni(COD)$_2$] (COD = 1,5-cyclooctadiene) in order to determine methods for clean installation. Product stereochemical outcomes are in some cases complicated and have been determined by NMR spectroscopic and crystallographic means. Density functional theory optimizations and accurate DLPNO-CCSD(T) energy calculations were also performed to support structural assignment.

INTRODUCTION

As a frontier of ligand design, secondary coordination sphere (SCS) ligand effects continue to capture great attention, translating lessons learned from enzymology to molecular-scale chemistry.[1,2,3,4] The installation of such peripheral groups has been the subject of a recent review, encompassing hydrogen-bond donors and acceptors, crown ethers, charged/redox-active groups, and Lewis acids, to name a few.[5] These lines of inquiry are guided beyond the primary coordination sphere (atoms directly connected to a metal) and encompass the use of non-covalent interactions to stabilize reactive substrates, alter redox behaviour, or shuttle reagents, as classic applications. As a point of emphasis, peripheral Lewis acids have been shown to i) stabilize Lewis bases, increasing concentrations at a metal active site, ii) alter the physiochemical properties of a coordinated amine e.g., pK_a tuning, iii) generate labile ligand precursors, and iv) serve as an acceptor site for hydride and nucleophile transfer.[6]

Efforts in our laboratory, and that of others,[7,8,9,10] have steered toward the synthesis of novel ligands having SCS boron groups. In 2020, we described the synthesis of 1,2-*bis*(di(3-dicyclohexylpropylboranyl)phosphino)-ethane – a diphosphine containing four projecting sp^2-hybridized borane units.[11] As a decoordinated species, this moiety bears two P—B interactions that by density functional theory, are calculated to provide 22 kcal mol^{-1} in stabilization.[12] A role for SCS boron groups was demonstrated using the nickel(0) compound, [Ni^0($P_2B^{Cy}_4$)$_2$] – a *bis*(diphosphine) compound that promotes the oxidative addition of iodoarenes (ArI) to give [Ni^{II}($P_2B^{Cy}_4$)(Ar)(I)] (**Chart 1A**).[13] By contrast, and consistent with previous literature precedent, the *n*-propyl derivative, [Ni(d*n*ppe)$_2$] (d*n*ppe = 1,2-*bis*(di-*n*-propylphosphino)ethane) displayed no such reactivity, pointing to an important role for $P_2B^{Cy}_4$ as a labile ligand precursor. These initial studies concerned *tetra*-substituted variants owing to ease in synthesis of the tetrakisallylphosphinoethane (tape) precursor, obtained by reaction of 1,2-*bis*(dichlorophosphino)ethane with excess allyl magnesium chloride. As a furtherance to these studies, we wished to expand the breadth of our program toward diphosphine ligands bearing fewer than four boranes in the SCS (**Chart 1B**). We reasoned that providing each phosphine arm with one pendant borane group would serve as a reasonable next step, reducing the number of boranes two-fold, while also providing an entrypoint into stereogenic phosphines that maintain a single P-B interaction in the decoordinated ligand precursor. The results of this endeavour are described herein.

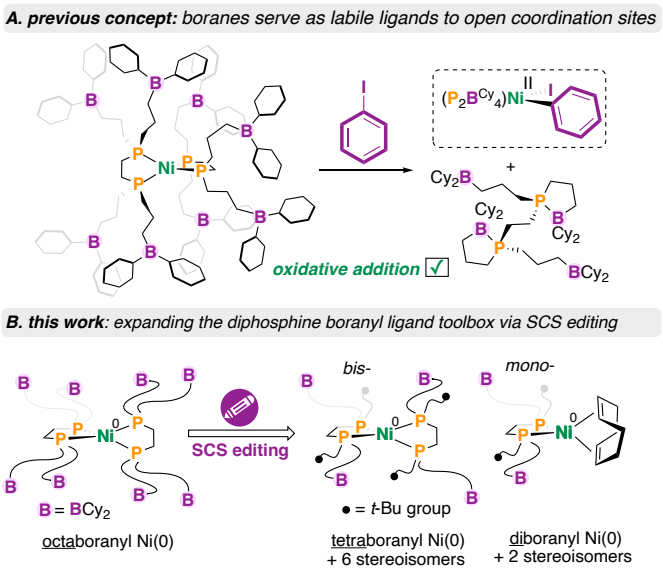

Chart 1. Expanding pendant-borane diphosphine-containing ligand space.

RESULTS AND DISCUSSION

The field of unsymmetric diphosphine ligand synthesis is shaped by challenges inherent to regio- and enantioselective installation of *R*-substituent.[14,15,16,17] Some early literature precedent, however, suggested the ability to selectively mono-functionalize 1,2-*bis*(dichlorophosphino)ethane (**1**) using larger cyclohexyl- or *tert*-butyl-substituted Grignard reagents, providing access to 1,2-*bis*-((chloro)alkyl)phosphino)ethane as a mixture of three (two racemic and one meso) isomers.[18] Although this pathway provides a mixture of chirogenic diphosphines, it nonetheless presents a practical means (and an initial testing ground) to access pendant diboranyl-containing diphosphine ligands. To our knowledge, these precursors have not been previously used to prepare diphosphine ligand precursors. Thus, reaction of **1** with *tert*-butyl magnesium chloride at -78 °C provided (±)-*rac*/*meso*-**2** as a white solid in 77% yield (1:0.75 mixture of isomers); Newman projections accompany each structure to clarify structural conformation (**Scheme 1**). The identity of the major isomer ((±)-*rac* or -*meso*) is unknown, but is likely the more stable (±)-*rac*-isomer.[18] For this and other diphosphine moieties described herein, ^{31}P NMR spectroscopy was used to determine the relative ratio of isomers (*e.g.*, δ_P = 130.6 and 128.0 ppm for (±)-*rac*/*meso*-**2**). Density functional theory (DFT)[19] optimizations were also performed; DLPNO-CCSD(T) calculations[20] provide a negligible (ΔG_{rel} = 1.7 kcal mol^{-1}) energetic difference between (±)-*rac*- and *meso*-**2**, consistent with observation of both. Subsequent reaction of (±)-*rac*/*meso*-**2** with allyl magnesium chloride allowed for preparation of the targeted ligand precursor, (±)-*rac*/*meso*-**3** ($P_2^{t\text{-BuAll}}$) as a viscous oil in 69% yield (1:0.87 ratio of isomers). Characteristic of P—Cl bond alkylation and trialkyl phosphine formation, a new pair of phosphorus signals was observed for (±)-*rac*/*meso*-**3** at δ_P = 1.99 and 1.78 ppm. The ^{1}H NMR spectrum of (±)-*rac* and *meso*-**3** additionally provided evidence for two isomers with signals in the allyl C(sp^2/sp^3)-H and ^{t}Bu regions, as appropriate (see ESI†). By DLPNO-CCSD(T), (±)-*rac*/*meso*-**3** were calculated to be near-identical in energy (ΔG_{rel} = 1.2 kcal mol^{-1}) (**Scheme 1**). To assess structural characteristics of the de-coordinated diboranyl diphosphine ligand, (±)-*rac*/*meso*-**3** was hydroborated using a stable monohydroborane, $HBCy_2$ (Cy = cyclohexyl),[21] which delivered a mixture of (±)-*rac*/*meso*-**4** (**Scheme 1**). ^{31}P NMR spectroscopy confirmed cyclization to give two five-

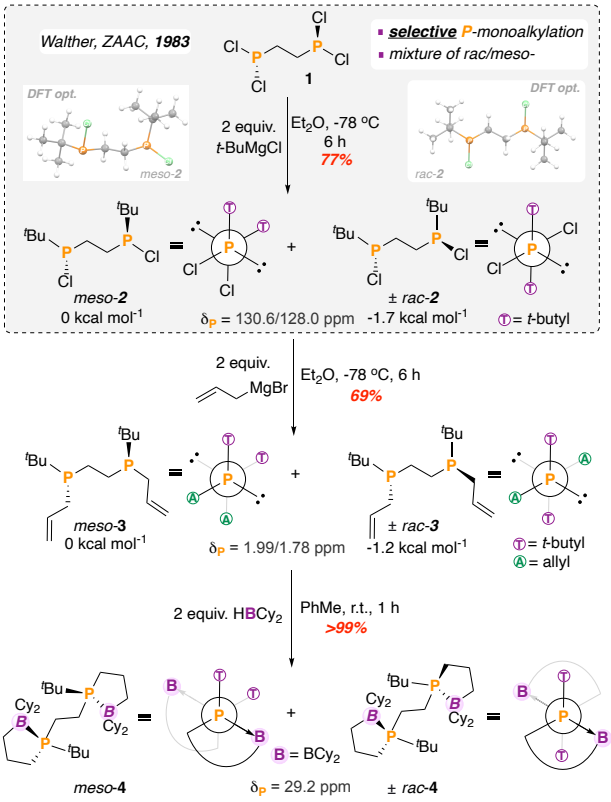

Scheme 1. Accessing the diphosphine ligand precursors **3** and **4**. Inset shows the DFT-optimized structures of *meso*- and (±)-*rac*-**2**. Product ratios described in the text.

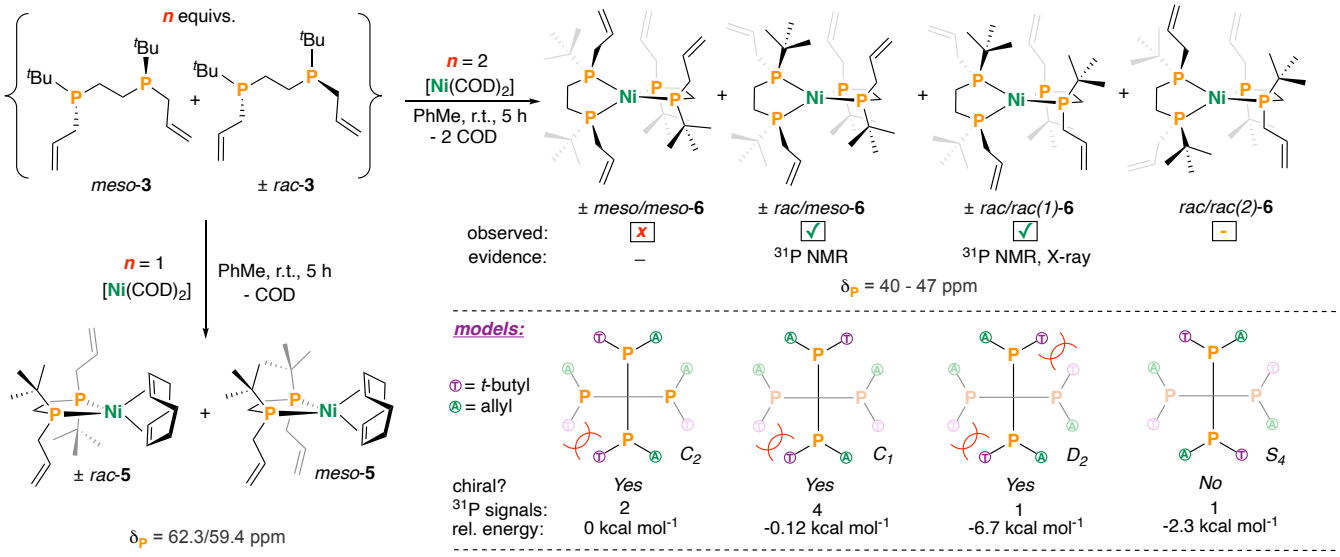

Scheme 2. Accessing the nickel(0) compounds (±)-*rac*/*meso*-**5** and isomers of **6**. Product ratios described in the text. A = allyl, T = *t*-Bu.

membered boron rings with a broad downfield-shifted signal at δ_P = 29.2 ppm (coincident for all isomers), similar to $P_2B^{Cy}{}_4$ (δ_P = 14.4 ppm),[11] while ^{11}B NMR spectroscopy gave a signature for the two sp^3-hybridized boranes at δ_B = +4.0 ppm ($\Delta_{1/2} \approx$ 550 Hz). Finally, a single X-ray diffraction experiment confirmed the structure of **4** with d(B—P) = 2.073(2) Å (**Figure 3**).

With routes to ligand precursor (±)-*rac/meso*-**3** established, we next targeted coordination to nickel(0). Reaction of (±)-*rac/meso*-**3** with [Ni(COD)$_2$] (COD = 1,5-cyclooctadiene) produced a dark brown solution, from which (±)-*rac/meso*-[Ni(P$_2$$^{t\text{-BuAll}}$)(COD)] ((±)-*rac/meso*-**5**) was isolated as an orange solid (**Scheme 2**). By ^{31}P NMR spectroscopy, signals at δ_P = 62.3 and 59.4 ppm were observed, consistent with two isomers in a 1:0.72 ratio. This result contrasts with the tetraallyl-ligand, tape where efforts to selectively prepare '[Ni(tape)(COD)]' were accompanied by considerable amounts of precipitate.[11] The DFT-optimized structure of both isomers is provided in **Figure 1**.

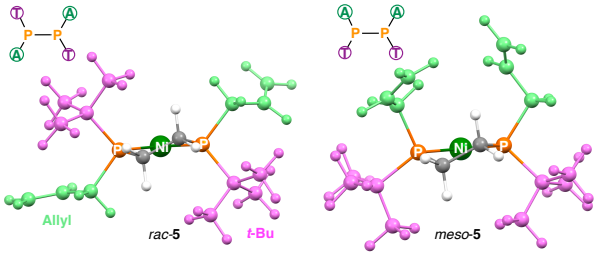

Figure 1. Rear-view of the DFT-computed structures of (±)-*rac/meso*-**5**; cyclooctadiene ligand omitted for clarity. A = allyl, T = *t*-Bu.

Isomers of the *bis*-diphosphine compounds, [Ni(P$_2$$^{t\text{-BuAll}}$)$_2$] (**6**) were also prepared by either treatment of a) (±)-*rac/meso*-**5** with 1 equiv. (±)-*rac/meso*-**3** or b) [Ni(COD)$_2$] with 2 equivs. of (±)-*rac/meso*-**3**. Based on the stereogenic nature of (±)-*rac/meso*-**3**, three chiral pairs and one achiral isomer (7 isomers total) could, in theory, be generated: three C_2-symmetric isomers, (±)-*meso/meso*-***6*** (point group = C_2), (±)-*rac/rac(1)*-***6*** (point group = D_2), as well as

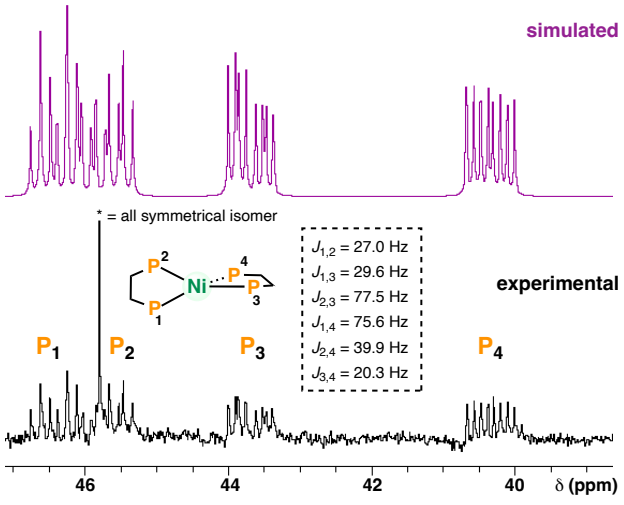

Figure 2. ^{31}P NMR spectrum (203 MHz, C_6D_6, 298 K) of **6**, showing two major isomers.

rac/rac(2)-**6** (point group = S_4), in addition to an enantiomeric pair of C_1-symmetric isomers, (±)-*rac/meso*-**6** (**Scheme 2**). Based on symmetry, a single ^{31}P NMR resonance was observed at δ_P = 45.7, assigned to (±)-*rac/rac(1)*-***6*** (confirmed by X-ray crystallography, *vide infra*), whereas four distinct doublets of doublets of doublets (ddd) (an ABXY spin-system) were observed for (±)-*rac/meso*-**6** in the range of δ_P = 40-47 ppm (*c.f.*, δ_P = 30.3 ppm for [Ni(tape)$_2$])[11] (see ESI†); these were observed in a 0.15:1 ratio. The observed and simulated ^{31}P NMR spectrum, obtained using DAISY simulation software,[22] are shown in **Figure 2**. Based on this data, (±)-*meso/meso*-**6** and *rac/rac*(2)-**6** which would be expected to provide 2 triplets and a singlet, respectively, were not observed.[23] DFT was additionally employed to provide structures of all isomers of **6.**

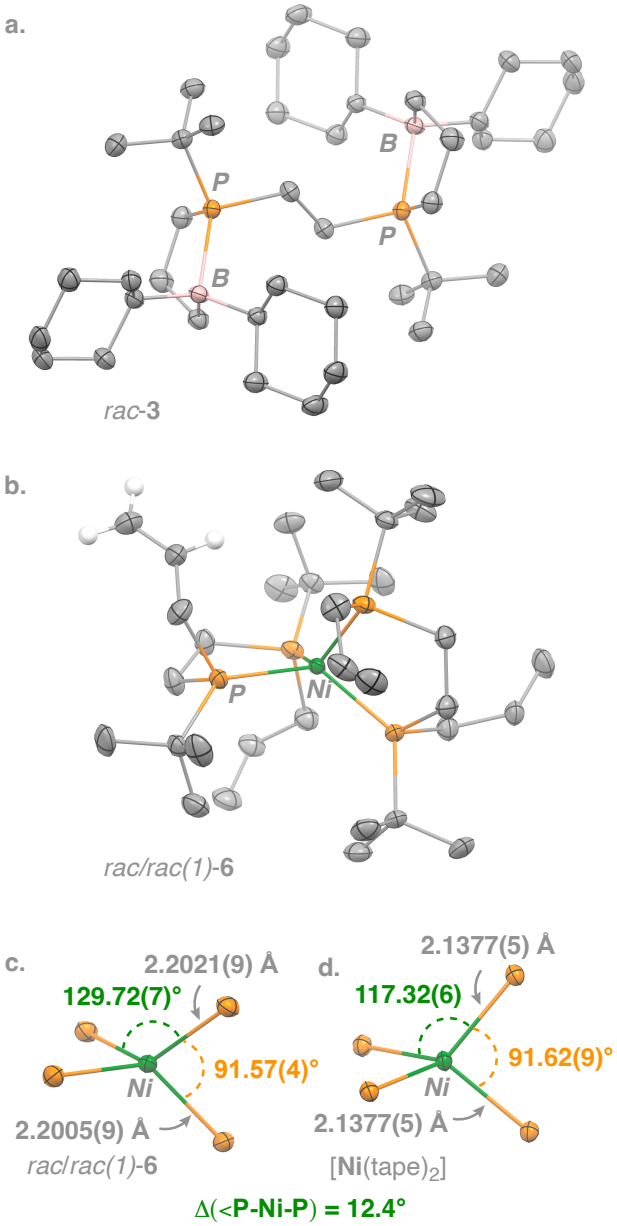

Figure 3. Mercury depiction of the solid-state molecular structure of **a**. *rac*-**3**, **b**. *rac/rac(1)*-**6** **c**. primary coordination sphere of *rac/rac(1)*-**6**, and **d**. primary coordination sphere of [Ni(tape)$_2$][11] (displacement ellipsoids are shown at the 50% probability, hydrogens omitted for clarity).

Consistent with our ability to obtain its solid-state structure, DLPNO-CCSD(T) calculations show that (±)-*rac/rac(1)*-**6** is the lowest energy isomer with G_{rel} = -6.7 kcal mol^{-1} compared to the highest energy conformer and ΔG_{rel} = 4.4 kcal mol^{-1} compared to *rac/rac(2)*-**6**. Of the *meso*-containing isomers, (±)-*rac/meso*-**6** was found to be 0.12 kcal mol^{-1} more stable than (±)-*meso/meso*-**6** (roughly equal).

Allowing a saturated toluene solution of **6** to evaporate at room temperature provided yellow blocks suitable for single-crystal X-ray diffraction analysis (**Figure 3**). The dataset features the *rac/rac(1)*- stereoisomer having a distorted tetrahedral Ni(0) center. When compared to the tetrakisallyl analogue, [Ni(tape)$_2$], *rac/rac(1)*-**6** contains a diphosphine ligand that is rotated by 14.4° (likely to avoid unfavourable *t*-Bu/*t*-Bu interactions). The incorporation of *t*-Bu groups also manifests in Ni—P bond lengthening by 3% as compared to [Ni(tape)$_2$][11] (from 2.137(2) to 2.200(1) Å) (**Figure 3**). For reference, compounds of the type, [M(dtbpe)$_2$] (dtbpe = 1,2-*bis*(di-*t*-butylphosphino)ethane) are not known,[24] presumably due to steric contraints imposed by the ligand *t*-Bu groups. This data confirms that the ^{31}P NMR signature at δ_P = 45.7 is due to *rac/rac(1)*-**6**.

Remote hydroboration was next targeted using HBCy$_2$. As a starting point, isomers of **5** were reacted with HBCy$_2$, providing two major singlets at δ_P = 66.2 and 63.6 ppm by ^{31}P NMR spectroscopy associated with formation of (±)-*rac/meso*-[Ni^0(P$_2$$^{t\text{-Bu}}B^{Cy}_2$)(COD)] ((±)-*rac/meso*-**7**) (**Scheme 3A**). This reaction, however, was not clean, and other species were observed by ^{31}P NMR spectroscopy (~34% purity; see ESI†). Previously, we showed that the tetraboranyl compound, P$_2$B^{Cy}$_4$ could be ring-opened in low conversion (14%) to give [Ni(P$_2$B^{Cy}$_4$)$_2$], albeit requiring forcing conditions (4 days, 70 °C); "[Ni(P$_2$B^{Cy}$_4$)(COD)]" was never observed (**Scheme 3B**).[11] We thus wondered if the bulkier P$_2$$^{t\text{-Bu}}B^{Cy}_2$ (**3**) derivative would show differential ring-opening behavior, owing to its bulkier *t*-Bu P-substituent. As proof of concept, exposure of (±)-*rac/meso*-**3** to [Ni(COD)$_2$] immediately resulted in *clean* formation of (±)-*rac/meso*-**7** (**Scheme 3A**). By ^{11}B NMR spectroscopy, a single broad resonance at δ_B = + 83.0 ($\Delta_{1/2}$ = 1100 Hz) was observed for both isomers. The structure of *rac*-**7** was also determined by X-ray crystallography and is depicted in **Figure 4.**

Highlighting steric bulk, efforts to hydroborate the pendant alkenes of **6** (all isomers) using HBCy$_2$ to give isomers of a *bis*(diboranyldiphosphine) Ni(0) compound **8** were unsuccessful (**Scheme 3C**). Instead, the expelled ligand, **4** was obtained (δ_P = 29.2 ppm); this reaction is balanced by loss of free 'Ni(0)'. Presumably, **4** results from hydrofunctionalization followed by ligand dissociation. By contrast, eight-fold hydroboration of [Ni(tape)$_2$] using HBCy$_2$ cleanly provides [Ni(P$_2$B^{Cy}$_4$)] where the ligand remains coordinated to Ni(0),[11] highlighting the difference between P$_2$$^{t\text{-Bu}}B^{Cy}_2$ and P$_2$B^{Cy}$_4$ (**Scheme 3D**). In summary, the bulky nature of P$_2$$^{t\text{-Bu}}B^{Cy}_2$ allows for facile P—B bond insertion to give [Ni(diphosphine)(COD)] yet disfavors formation of [Ni(diphosphine)$_2$]. By contrast, P$_2$B^{Cy}$_4$ disfavors P—B insertion and allows for access to [Ni(diphosphine)$_2$].

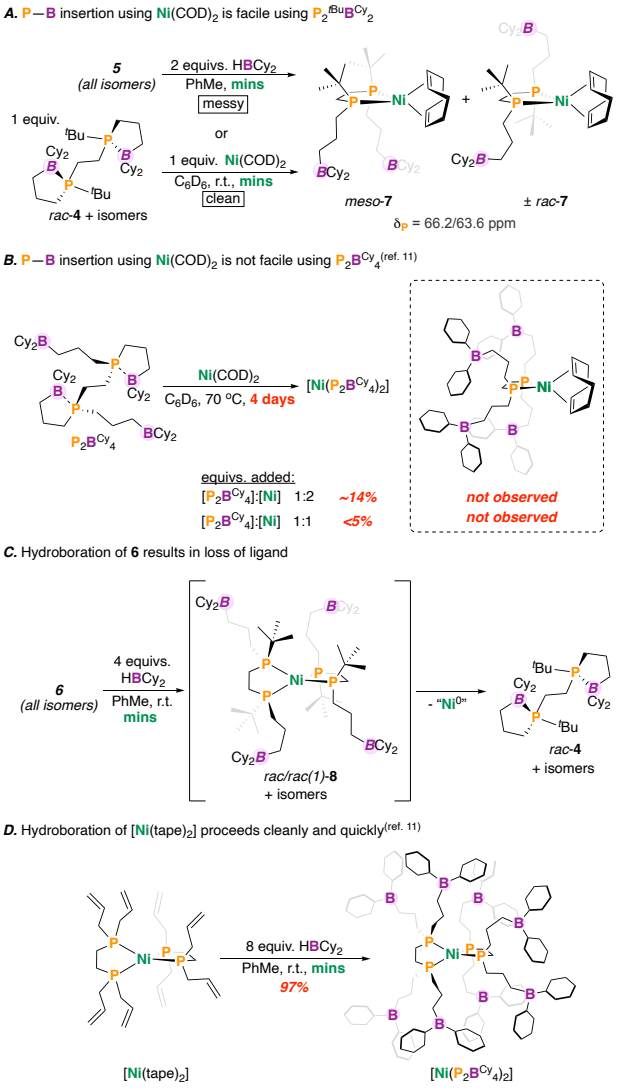

Scheme 3. Hydroboration of isomers **5** and **6** using HBCy$_2$.

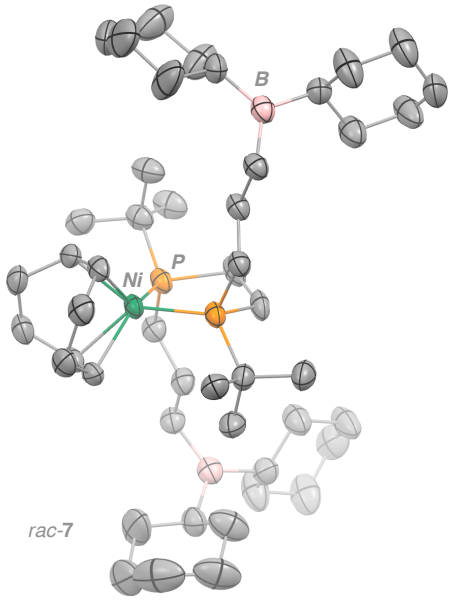

Figure 4. Mercury depiction of the solid-state molecular structure of *rac*-**7** (displacement ellipsoids are shown at the 50% probability, hydrogens omitted for clarity).

CONCLUSION

In sum, we have exposed (±)-*rac*/*meso*-(*t*-Bu)ClP-CH_2CH_2-PCl(*t*-Bu) as a valuable precursor to facilely access diboranyl diphosphine ligands. Comparison of the tetraboranyl ($P_2B^{Cy}_4$) and diboranyl ($P_2{}^{t\text{-Bu}}B^{Cy}_2$) analogues reveal stark coordination differences including facile ligand loss from presumed '[Ni($P_2{}^{t\text{-Bu}}B^{Cy}_2$)$_2$]' as well as rapid phosphorus-boron bond insertion into $P_2{}^{t\text{-Bu}}B^{Cy}_2$ to give [Ni($P_2{}^{t\text{-Bu}}B^{Cy}_2$)(COD)]. As described above, these qualities are unique to this ligand class. Overall, this report offers a blueprint for the synthesis of diboranyldiphosphines and cements a rigorous spectroscopic and computational foundation from which future ligand generations will be developed. We are particularly interested in designing routes into enantiopure di- and monoboranyldiphosphines – an aim that is currently underway.

EXPERIMENTAL DATA

General Considerations. All experiments were carried out employing standard Schlenk techniques under an atmosphere of dry nitrogen employing degassed, dried solvents in a solvent purification system supplied by PPT, LLC. Non-halogenated solvents were tested with a standard purple solution of sodium benzophenone ketyl in tetrahydrofuran to confirm effective moisture removal. d_6-benzene was dried over molecular sieves and degassed by three freeze-pump-thaw cycles. $HBCy_2$[21] was prepared using literature procedures. All other reagents were purchased from commercial vendors and used without further purification unless otherwise stated.

Physical methods. ^{1}H NMR spectra are reported in parts per million (ppm) and are referenced to residual solvent e.g., ^{1}H(C_6D_6): δ 7.16; ^{13}C(C_6D_6): 128.06; coupling constants are reported in Hz. ^{13}C, ^{11}B, and ^{31}P NMR spectra were performed as proton-decoupled experiments and are reported in ppm.

Preparation of Compounds.

Note: All compounds were isolated as mixtures of isomers ((±)-*rac*/*meso*). Data is listed for Major and Minor isomers; ratios were determined by ^{31}P NMR spectroscopy. In cases were overlap was determined, signals are provided as "Both isomers".

(±)-*rac*/*meso*-1,2-*bis*-((chloro)*tert*-butyl)phosphino)ethane[18] [CAS: 89227-46-3] ((±)-*rac*/*meso*-**2**; $C_{10}H_{22}Cl_2P_2$, M_W = 274 g/mol): In the glovebox, $Cl_2P(CH_2)_2PCl_2$ (1.29 g, 0.0056 mol) was added to a 250 mL reaction flask equipped with a stir bar and 100 mL Et_2O. The reaction flask was cycled onto a Schlenk line and *tert*-butylmagnesium chloride (5.6 mL, 0.011 mol, 2 equiv.) was added dropwise at -78 °C. This mixture was warmed to room temperature and stirred for 6 h. Next, the resulting white cloudy solution was filtered and dried *in-vauco* affording (±)-*rac*/*meso*-**2** as a white solid (1.19 g, 77%). **^{1}H{^{31}P} NMR (500 MHz, C_6D_6, 298 K):** Major Isomer: δ_H = 2.09 (m; CH_2), 1.96 (m; CH_2), 0.91 (s; *t*-Bu). Minor Isomer: δ_H = 2.20 (m; CH_2), 1.74 (m; CH_2), 0.93 (s; *t*-Bu). **^{13}C{^{1}H} NMR (125.8 MHz, C_6D_6, 298 K):** Major isomer: δ_C = 32.8 (m), 26.9 (d, $J_{C,P}$ = 19.1 Hz; *t*-Bu), 25.2 (d, $J_{C,P}$ = 8.1 Hz; *t*-Bu). Minor isomer: δ_C = 33.1 (m), 26.6 (d, $J_{C,P}$ = 19.5 Hz; *t*-Bu), 25.3 (d, $J_{C,P}$ = 8.0 Hz; *t*-Bu). **^{31}P{^{1}H} NMR (202.5 MHz, C_6D_6, 298 K):** δ_P = + 130.6 (Major isomer; integration: 1.00), +128.0 (Minor isomer; rel. integration: 0.75).

(±)-*rac*/*meso*-1,2-*bis*-((allyl)*tert*-butyl)phosphino)ethane ((±)-*rac*/*meso*-**3**; $\mathbf{P_2}^{t\text{-Bu,All}}$, $C_{16}H_{32}P_2$, M_W = 286 g/mol): In the glovebox, (±)-*rac*/*meso*-**2** (500 mg, 1.82 mmol) was added to a 250 mL reaction flask equipped with a stir bar and 100 mL Et_2O. The reaction flask was cycled onto a Schlenk line and allylmagnesium chloride (1.82 mL, 3.63 mmol, 2 equiv.) was added dropwise at -78 °C. This mixture was warmed to room temperature and stirred for 6 h. A saturated degassed brine solution (30 mL) was next added to the reaction mixture. The organic layer was filtered into a Schlenk tube containing $MgSO_4$ to remove residual water. The solution was subsequently filtered and dried *in-vauco* affording (±)-*rac*/*meso*-**3** as a pale-yellow oil (358 mg, 69%). **^{1}H{^{31}P} NMR (500 MHz, C_6D_6, 298 K):** δ_H = 5.96 (m, CH(allyl); Both isomers), 5.05 (m, CH_2(allyl); Both isomers), 4.98 (m, CH_2(allyl); Both isomers), 2.26 (m, CH_2(allyl); isomer 1), 2.23 (m, CH_2(allyl); Major isomer), 2.12 (m, CH_2(allyl); Major isomer), 2.09 (m, CH_2(allyl); Minor isomer), 1.63 (m, CH_2(linker); Both isomers), 0.98 (s, *t*-Bu; Major isomer), 0.97 (s, *t*-Bu; Minor isomer). **^{13}C{^{1}H} NMR (125.8 MHz, C_6D_6, 298 K):** δ_C = 136.4 (m, C(allyl); Both isomers), 115.8 (m, C(allyl); Both isomers), 31.0 (m; CH_2(linker); Both isomers), 28.4 (m, t-Bu; Both isomers), 27.7 (d, $J_{P,C}$ = 6.7 Hz, *t*-Bu; Minor isomer), 27.6 (d, $J_{P,C}$ = 6.8 Hz, *t*-Bu; Major isomer), 22.5 (m, C(allyl); Major isomer), 22.3 (m, C(allyl); Minor isomer). **^{31}P{^{1}H} NMR (202.5 MHz, C_6D_6, 298 K):** δ_P = + 1.99 (Minor isomer; rel. integration: 0.87), +1.78 (Major isomer; integration: 1.00).

(±)-*rac*/*meso*-1,2-*bis*-((3-dicyclohexylboranyl)propyl)*tert*-butyl)phosphino)ethane ((±)-*rac*/*meso*-**4**; $\mathbf{P_2}^{t\text{-Bu}}\mathbf{B}^{Cy}_2$, $C_{40}H_{78}B_2P_2$, M_W = 642 g/mol): In the glovebox, $\mathbf{P_2}^{t\text{-Bu,All}}$ ((±)-*rac*/*meso*-**2**) (20 mg, 0.070 mmol) and $HBCy_2$ (25 mg, 0.14 mmol, 2 equiv.) were combined in a 20 mL scintillation vial equipped with a stir bar. Approximately 1 mL of toluene was added, and the solution was allowed to stir for 10 min at room temperature. Removal of solvent *in-vacuo* and recrystallization from hexanes gave (±)-*rac*/*meso*-**4** as a white solid (22 mg, 49%). **^{1}H{^{31}P} NMR (500 MHz, C_6D_6, 298 K):** δ_H = 1.98 (m, 8H), 1.90 (m, 8H), 1.77 (m, 8H), 1.66 (m, 8H), 1.56-1.25 (overlapping m, 22H), 1.10 (m, 2H), 0.98 (s, 18H; *t*-Bu), 0.74 (m, 4H). *N.B.* All signals overlap for Both isomers. **^{13}C{^{1}H} NMR (125.8 MHz, C_6D_6, 298 K):** δ_C = 34.6 (m), 33.8 (m), 33.3 (m), 30.4 (m), 30.1, 29.9, 28.0, 27.6, 21.8 (m), 19.7 (m). **^{31}P{^{1}H} NMR (202.5 MHz, C_6D_6, 298 K):** δ_P = 29.2 (s, overlapping for Both isomers). **^{11}B{^{1}H} NMR (160.5 MHz, C_6D_6, 298 K):** δ_B = + 4.02 ($\Delta_{1/2}$ = 550 Hz).

(±)-*rac/meso*-[Ni⁰(P₂$^{t\text{-Bu,All}}$)(COD)] ((±)-*rac/meso*-**5**; $C_{24}H_{44}P_2Ni$, M_W = 452 g/mol): In the glovebox, [Ni⁰(COD)₂] (14.4 mg, 0.0523 mmol) and (±)-*rac/meso*-**3** (15 mg, 0.0523 mmol, 1 equiv.) were added to a 20 mL scintillation vial equipped with a stir bar containing 4 mL toluene. This mixture was stirred for 3 h and toluene removed *in-vauco*. The resulting crude product was dissolved in hexane and filtered. Some hexane was removed *in-vauco* to concentrate the mixture and the compound was left to crystalize at -35 °C giving (±)-*rac/meso*-**5** as yellow blocks (18 mg, 76%). **^{1}H{^{31}P} NMR (500 MHz, tol-d$_8$, 298 K):** δ_H = 5.74 (m, CH(allyl); Both isomers), 5.56 (m, CH(allyl); Both isomers), 5.06-4.75 (m, CH_2(allyl); Both isomers), 4.51 (m, CH(COD); Major isomer), 4.44 (m, CH(COD); Minor isomer), 4.24 (m, CH(COD); Minor isomer), 4.00 (m, CH(COD); Major isomer), 2.65-2.25 (m, CH_2(COD); Both isomers), 1.50-1.10 (overlapping CH_2(allyl) and P-CH_2; Both isomers), 1.08 (s, *t*-Bu; Major isomer), 1.01 (s, *t*-Bu; Minor isomer). **^{13}C{^{1}H} NMR (125.8 MHz, tol-d$_8$, 298 K):** δ_C = 136.0 (C(allyl); Major isomer), 135.6 (C(allyl); Minor isomer), 116.2 (C(allyl); Minor isomer), 115.4 (C(allyl); Minor isomer), 82.4 (CH(COD); Minor isomer), 81.5 (CH(COD); Major isomer), 78.8 ((CH(COD); Major isomer), 78.7 (CH(COD); Minor isomer), 34.9, 34.4 (m), 32.9 (m), 32.6, 32.4 (m), 32.3 (m), 30.3 (m), 27.6 (C-*t*-Bu), 27.4 (C-*t*-Bu), 24.1, 23.9, 23.8. *N.B.* Major and minor isomers are not assigned to C(sp^3)-H groups. **^{31}P{^{1}H} NMR (202.5 MHz, tol-d$_8$, 298 K):** δ_P = + 62.3 (Major isomer; integration: 1.00), 59.4 (Minor isomer; rel. integration: 0.72).

[Ni⁰(P₂$^{t\text{-Bu,All}}$)₂] (isomers of **6**; $C_{32}H_{64}NiP_4$, M_W = 630 g/mol): In the glovebox, [Ni(COD)₂] (20 mg, 0.073 mmol, 1 equiv.) and ((±)-*rac/meso*-**3**) (42 mg, 0.15 mmol, 2 equivs.) were added to a 20 mL scintillation vial equipped with a stir bar and 4 mL toluene. This mixture was stirred for 3 h and toluene removed *in-vauco*. The resulting crude product was dissolved in hexane and filtered. Some hexane was removed *in-vauco* and the compound was left to crystalize via slow evaporation giving isomers of **6** (30 mg, 66%). **^{1}H{^{31}P} NMR (500 MHz, C$_6$D$_6$, 298 K):** δ_H = 6.36-6.02 (m, CH(allyl); Both isomers), 5.15-4.93 (m, CH_2(allyl); Both isomers), 2.92-2.46 (m, CH_2(allyl); Both isomers), 1.94-1.65 (m, Both isomers), 1.32-1.21 (m, Both isomers), 1.26 (s, *t*-Bu; Major isomer), 1.23 (s, *t*-Bu; Minor isomer), 1.234 (s, *t*-Bu; Major isomer), 1.219 (s, *t*-Bu; Major isomer), 1.207 (s, *t*-Bu; Major isomer). **^{13}C{^{1}H} NMR (125.8 MHz, C$_6$D$_6$, 298 K):** δ_C = 135.6, 114.3, 37.7 (m), 31.5 (m), 28.4, 20.9 (m). Minor isomer only. **^{31}P{^{1}H} NMR (202.5 MHz, C$_6$D$_6$, 298 K):** δ_P = 45.7 (s; Minor isomer; rel. integration: 0.15), 46.40 (ddd, $J_{P,P}$ = 75.6 Hz, $J_{P,P}$ = 29.6 Hz, $J_{P,P}$ = 27.0 Hz; Major isomer; integration: 1.00), 45.65 (ddd, $J_{P,P}$ = 77.5 Hz, $J_{P,P}$ = 39.9 Hz, $J_{P,P}$ = 27.0 Hz; Major isomer; integration: 1.00), 43.68 (ddd, $J_{P,P}$ = 77.5 Hz, $J_{P,P}$ = 29.6 Hz, $J_{P,P}$ = 20.3 Hz; Major isomer; integration: 1.00), 40.33 (ddd, $J_{P,P}$ = 75.6 Hz, $J_{P,P}$ = 39.9 Hz, $J_{P,P}$ = 20.3 Hz; Major isomer; integration: 1.00).

(±)-*rac/meso*-[Ni⁰(P₂$^{t\text{-Bu}}$B^{Cy}₂)(COD)]: (*rac/meso*-**7**; $C_{48}H_{90}B_2P_2Ni$, M_W = 809 g/mol): **Route A:** In the glovebox, **(±)-*rac/meso*-[Ni⁰(P₂$^{t\text{-Bu,All}}$)(COD)]** ((±)-*rac/meso*-**5**) (31 mg, 0.068 mmol, 1 equiv.) and $HBCy_2$ (24 mg, 0.14 mmol, 2 equiv.) were combined in a 20 mL scintillation vial equipped with a stir bar. Approximately 1 mL of toluene was added, and the solution was allowed to stir for 10 min at room temperature. Removal of solvent *in-vacuo* and dissolution in C_6D_6 provided signals attributable to (±)-*rac/meso*-**7** along with other a series of impurities (34% purity by ^{31}P NMR spectroscopy). This route was not used to isolate (±)-*rac/meso*-**7**. **Route B:** In the glovebox, [Ni⁰(COD)₂] (18 mg, 0.07 mmol, 1 equiv.) and (±)-*rac/meso*-**4** (43 mg, 0.07 mmol, 1 equiv.) were added to a 20 mL scintillation vial equipped with a stir bar containing 4 mL toluene. This mixture was stirred for 20 mins and toluene removed *in-vauco*. The resulting crude product was dissolved in hexane and filtered. Some hexane was removed *in-vauco* to concentrate the mixture giving (±)-*rac/meso*-**7** as a yellow solid (41 mg, 76%). **^{1}H NMR (500 MHz, C$_6$D$_6$, 298 K):** δ_H = 4.69 (m, CH(COD); Major isomer), 4.63 (m, CH(COD); Minor isomer), 4.30 (m, CH(COD); Minor isomer), 4.10 (m, CH(COD); Major isomer), 2.79-2.19 CH_2(COD); Both isomers), 1.84-1.16 (m, overlapping CH_2(allyl), Cy, and P-CH_2; Both isomers), 1.24 (d, *t*-Bu; Major isomer). **^{13}C{^{1}H} NMR (125.8 MHz, C$_6$D$_6$, 298 K):** δ_C = 80.8 (CH(COD)), 78.6 (CH(COD)), 35.6, 34.5, 31.4, 30.1, 29.9, 27.5, 27.4, 27.1, 27.0, 24.5 (m). Major isomer only. **^{11}B{^{1}H} NMR (160.5 MHz, C$_6$D$_6$, 298 K):** δ_B = + 83.0 ($\Delta_{1/2}$ = 1100 Hz; Both isomers). **^{31}P{^{1}H} NMR (202.5 MHz, C$_6$D$_6$, 298 K):** δ_P = + 66.2 (Major isomer; integration: 1.00), 63.6 (Minor isomer; rel. integration: 0.18). *N.B.* These integrals are post re-crystallization.

[Ni⁰(P₂$^{t\text{-Bu}}$B^{Cy}₂)₂] (isomers of **8**; $C_{80}H_{156}B_4P_4Ni$, M_W = 1343 g/mol). **Attempted synthesis**: In the glovebox, **[Ni⁰(P₂$^{t\text{-Bu,All}}$)₂]** (isomers of **6**) (5 mg, 0.008 mmol, 1 equiv.) and $HBCy_2$ (6 mg, 0.03 mmol, 4 equiv.) were dissolved in 500 µL of C_6D_6 and transferred to a J. Young NMR tube. Analysis by ^{31}P NMR spectroscopy showed formation of (±)-*rac/meso*-**4** in *ca.* 64%.

ASSOCIATED CONTENT

Supporting Information

^{1}H, ^{13}C{^{1}H}, ^{31}P{^{1}H}, and ^{11}B NMR spectra for all complexes. XYZ coordinates for DFT calculations. CCDC **2174779-2174780** and **2182649** contain the supplementary crystallographic data for this paper. These data can be obtained free of charge from The Cambridge Crystallographic Data Centre *via* www.ccdc.cam.ac.uk/data_request/cif.

AUTHOR INFORMATION

Corresponding Author

*mdrover@uwindsor.ca

CONFLICTS OF INTEREST

There are no conflicts to declare.

ACKNOWLEDGEMENTS

The authors are grateful to the University of Windsor, the Council of Ontario Universities for a John C. Polanyi award to M.W.D., and the Natural Sciences and Engineering Research Council of Canada (Discovery Grant, RGPIN-2020-04480, Discovery Launch

Supplement, DGECR-2020-00183, and graduate award (OGS to B.J.H.A. and J.A.Z. and CGS-M/NSERC Vanier to J.A.Z.) for funding. This work was also made possible by the facilities of the Shared Hierarchical Academic Research Computing Network (SHARCNET:www.sharcnet.ca) and Compute/Calcul Canada.

REFERENCES & NOTES

(1) Nichols, A. W.; Machan, C. W. Secondary-Sphere Effects in Molecular Electrocatalytic CO_2 Reduction. *Front. Chem.* **2019**, *7*, 397.

(2) Thammavongsy, Z.; Mercer, I. P.; Yang, J. Y. Promoting Proton Coupled Electron Transfer in Redox Catalysts through Molecular Design. *Chem. Commun.* **2019**, *55* (70), 10342–10358.

(3) Mann, S. I.; Heinisch, T.; Ward, T. R.; Borovik, A. S. Coordination Chemistry within a Protein Host: Regulation of the Secondary Coordination Sphere. *Chem. Commun.* **2018**, *54* (35), 4413–4416.

(4) Lewis, J. C. Beyond the Second Coordination Sphere: Engineering Dirhodium Artificial Metalloenzymes To Enable Protein Control of Transition Metal Catalysis. *Acc. Chem. Res.* **2019**, *52* (3), 576–584.

(5) Drover, M. W. A Guide to Secondary Coordination Sphere Editing. *Chem. Soc. Rev.* **2022**, *51* (6), 1861–1880.

(6) Zurakowski, J. A.; Austen, B. J. H.; Drover, M. W. Exterior Decorating: Lewis Acid Secondary Coordination Spheres for Cooperative Reactivity. *Trends. Chem.* **2022**, *4*, 331–346.

(7) Kiernicki, J. J.; Norwine, E. E.; Zeller, M.; Szymczak, N. K. Tetrahedral Iron Featuring an Appended Lewis Acid: Distinct Pathways for the Reduction of Hydroxylamine and Hydrazine. *Chem. Commun.* **2019**, *55* (79), 11896–11899.

(8) Kiernicki, J. J.; Zeller, M.; Szymczak, N. K. Requirements for Lewis Acid-Mediated Capture and N–N Bond Cleavage of Hydrazine at Iron. *Inorg. Chem.* **2019**, *58* (2), 1147–1154.

(9) Miller, A. J. M.; Labinger, J. A.; Bercaw, J. E. Reductive Coupling of Carbon Monoxide in a Rhenium Carbonyl Complex with Pendant Lewis Acids. *J. Am. Chem. Soc.* **2008**, *130* (36), 11874–11875.

(10) Cowie, B. E.; Emslie, D. J. H. Bis-Hydrocarbyl Platinum(II) Ambiphilic Ligand Complexes: Alkyl–Aryl Exchange between Platinum and Boron. *Organometallics* **2015**, *34* (12), 2737–2746.

(11) Drover, M. W.; Dufour, M. C.; Lesperance-Nantau, L. A.; Noriega, R. P.; Levin, K.; Schurko, R. W. Octaboraneyl Complexes of Nickel: Monomers for Redox-Active Coordination Polymers. *Chem. Eur. J.* **2020**, *26* (49), 11180–11186.

(12) Zurakowski, J. A.; Bhattacharyya, M.; Spasyuk, D. M.; Drover, M. W. Octaboraneyl $[Ni(H)(Diphosphine)_2]^+$ Complexes: Exploiting Phosphine Ligand Lability for Hydride Transfer to an $[NAD]^+$ Model. *Inorg. Chem.* **2021**, *60* (1), 37–41.

(13) Zurakowski, J. A.; Austen, B. J. H.; Dufour, M. C.; Spasyuk, D. M.; Nelson, D. J.; Drover, M. W. Lewis Acid-Promoted Oxidative Addition at a $[Ni^0(Diphosphine)_2]$ Complex: The Critical Role of a Secondary Coordination Sphere. *Chem. Eur. J.* **2021**, *27* (64), 16021–16027.

(14) Chaux, F.; Frynas, S.; Laureano, H.; Salomon, C.; Morata, G.; Auclair, M.-L.; Stephan, M. (Massoud); Merdès, R.; Richard, P.; Ondel-Eymin, M.-J.; Henry, J.-C.; Bayardon, J.; Darcel, C.; Jugé, S. Enantiodivergent Synthesis of P-Chirogenic Phosphines. *Comptes Rendus Chimie* **2010**, *13* (8–9), 1213–1226.

(15) Imamoto, T.; Watanabe, J.; Wada, Y.; Masuda, H.; Yamada, H.; Tsuruta, H.; Matsukawa, S.; Yamaguchi, K. P-Chiral Bis(Trialkylphosphine) Ligands and Their Use in Highly Enantioselective Hydrogenation Reactions. *J. Am. Chem. Soc.* **1998**, *120* (7), 1635–1636.

(16) Hoge, G.; Wu, H.-P.; Kissel, W. S.; Pflum, D. A.; Greene, D. J.; Bao, J. Highly Selective Asymmetric Hydrogenation Using a Three Hindered Quadrant Bisphosphine Rhodium Catalyst. *J. Am. Chem. Soc.* **2004**, *126* (19), 5966–5967.

(17) Hoge, G. Synthesis of Both Enantiomers of a P-Chirogenic 1,2-Bisphospholanoethane Ligand via Convergent Routes and Application to Rhodium-Catalyzed Asymmetric Hydrogenation of CI-1008 (Pregabalin). *J. Am. Chem. Soc.* **2003**, *125* (34), 10219–10227.

(18) Weisheit, R.; Stendel, R.; Messbauer, B.; Langer, C.; Walther, B. Synthese von Bis(tert.-butylphosphino)ethan, $Bu^tHPCH_2CH_2PHBu^t$, und 1-tert.-Butylphosphino-2-diphenylphosphino-ethan, $Ph_2PCH_2CH_2PHBu^t$, sowie deren sekundre Phosphinchalkogenide. *Z. Anorg. Allg. Chem.* **1983**, *504* (9), 147–154.

(19) Gaussian 16, Revision C.01, M. J. Frisch, G. W. Trucks, H. B. Schlegel, G. E. Scuseria, M. A. Robb, J. R. Cheeseman, G. Scalmani, V. Barone, G. A. Petersson, H. Nakatsuji, X. Li, M. Caricato, A. V. Marenich, J. Bloino, B. G. Janesko, R. Gomperts, B. Mennucci, H. P. Hratchian, J. V. Ortiz, A. F. Izmaylov, J. L. Sonnenberg, D. Williams-Young, F. Ding, F. Lipparini, F. Egidi, J. Goings, B. Peng, A. Petrone, T. Henderson, D. Ranasinghe, V. G. Zakrzewski, J. Gao, N. Rega, G. Zheng, W. Liang, M. Hada, M. Ehara, K. Toyota, R. Fukuda, J. Hasegawa, M. Ishida, T. Nakajima, Y. Honda, O. Kitao, H. Nakai, T. Vreven, K. Throssell, J. A. Montgomery, Jr., J. E. Peralta, F. Ogliaro, M. J. Bearpark, J. J. Heyd, E. N. Brothers, K. N. Kudin, V. N. Staroverov, T. A. Keith, R. Kobayashi, J. Normand, K. Raghavachari, A. P. Rendell, J. C. Burant, S. S. Iyengar, J. Tomasi, M. Cossi, J. M. Millam, M. Klene, C. Adamo, R. Cammi, J. W. Ochterski, R. L. Martin, K. Morokuma, O. Farkas, J. B. Foresman, and D. J. Fox, Gaussian, Inc., Wallingford CT, 2016.

(20) A) Riplinger, C.; Neese, F. *J. Chem. Phys.* **2013**, 138, No. 034106; b) Riplinger, C.; Pinski, P.; Becker, U.; Valeev, E. F.; Neese, F. *J. Chem. Phys.* **2016**, 144, No. 024109; c) Riplinger, C.; Sandhoefer, B.; Hansen, A.; Neese, F. *J. Chem. Phys.* **2013**, *139*, 134101; d) Neese, F. *WIREs Comput. Mol. Sci.* **2012**, *2*, 73; e) Neese, F. *WIREs Comput. Mol. Sci.* **2018**, *8*, No. E1327.

(21) Atsushi, A. Dicyclohexylboron Trifluoromethanesulfonate. *Org. Synth.* **2002**, *79*, 103.

(22) Daisy, Topspin 2.0.

(23) We cannot exclude the possibility that a signal for (±)-*rac*/*rac*(2)-**6** could be coincident with those noted for (±)-*rac*/*meso*-**6** and (±)-*rac*/*rac*(1)-**6**.

(24) Based on a Scifinder Search, April 2022.